

# Fixed-Order H-Infinity Controller Design for Port-Hamiltonian Systems<sup>\*,\*\*</sup>

Paul Schwerdtner<sup>a,\*</sup>, Matthias Voigt<sup>b</sup>

<sup>a</sup>*TU Berlin, Institute of Mathematics, Straße des 17. Juni 136, 10623 Berlin, Germany*

<sup>b</sup>*UniDistance Suisse, Schinerstrasse 18, 3900 Brig, Switzerland*

## Abstract

We present a new fixed-order H-infinity controller design method for potentially large-scale port-Hamiltonian (pH) plants. Our method computes controllers that are also pH (and thus passive) such that the resulting closed-loop systems is again passive, which ensures closed-loop stability simply from the structure of the plant and controller matrices. In this way, we can avoid computationally expensive eigenvalue computations that would otherwise be necessary. In combination with a sample-based objective function which allows us to avoid multiple evaluations of the H-infinity norm (which is typically the main computational burden in fixed-order H-infinity controller synthesis), this makes our method well-suited for plants with a high state-space dimension.

In our numerical experiments, we show that applying a passivity-enforcing post-processing step after using well-established H-infinity synthesis methods often leads to a deteriorated H-infinity performance. In contrast to that, our method computes pH controllers, that are automatically passive and simultaneously aim to minimize the H-infinity norm of the closed-loop transfer function. Moreover, our experiments show that for large-scale plants, our method is significantly faster than the well-established fixed-order H-infinity controller synthesis methods.

**Keywords:** port-Hamiltonian systems, large-scale systems, robust control, H-infinity control, fixed-order controllers

## 1. Introduction

The port-Hamiltonian (pH) modeling paradigm is used for energy-based modeling of complex processes across several physical domains including electrical systems (Mehrmann et al., 2018), flow-problems (Hauschild et al., 2020), and mechanical multi-body systems (Beattie et al., 2018, Example 12). The two main benefits of pH models are the intuitive energy-based interconnection of systems from different physical domains and the beneficial properties such as *passivity* that follow directly from the model structure. In recent years, the increased demand for accurate models of complex multi-physical processes has led to a wide-spread utilization of pH models and subsequently system theoretical tools such as model order reduction and system identification have been adapted to pH systems; see Mehrmann and Unger (2022) for an overview of recent methods and applications. The available pH controller design strategies developed in Ortega et al. (2008); Ramirez et al. (2016); Zhang et al. (2017) are

mostly based on energy-shaping and do not aim for classical  $\mathcal{H}_2$  or  $\mathcal{H}_\infty$  optimal controllers. In this work, we present a new algorithm for fixed-order  $\mathcal{H}_\infty$  controller design for pH systems.

Well-established numerical methods for classical  $\mathcal{H}_\infty$  controller design are based on the repeated solution of linear matrix inequalities (LMIs) or algebraic Riccati equations (AREs); see, e.g., the monographs Francis (1987); Zhou et al. (1996); Skogestad and Postlethwaite (2005). The AREs are often solved using structured generalized eigenvalue problems (Benner et al., 2002, 2011). LMI- or ARE-based control is widely used for plants with small state-dimension (also called plant *order*). The main drawback of these methods is that the obtained controllers have the same order as the plant (and are thus often called *full-order* controllers). This is undesired for plants with higher order, since the implementation of high controllers is often impractical. For some system classes, low-rank solvers for AREs have enabled the computation of low-order controllers (Benner et al., 2022). Otherwise, a subsequent *controller order reduction* is necessary (Mustafa and Glover, 1991; Anderson and Liu, 1989). Note that full-order ARE-based  $\mathcal{H}_\infty$  control for pH systems is currently under investigation; see Breiten and Karsai (2022) for a recent preprint.

In the early 2000s, *fixed-order*  $\mathcal{H}_\infty$  controller synthesis methods have been established, in which the set of controllers of a fixed and typically low order is parameterized and then the controller pa-

\*This research has been supported by the German Research Foundation (DFG) within the project 424221635.

\*\***CRedit author statement:** Paul Schwerdtner Conceptualization, Methodology, Software, Data Curation, Writing – Original Draft, Visualization, Matthias Voigt: Conceptualization, Writing – Review & Editing, Supervision, Funding Acquisition

\*Corresponding author.

Email addresses: schwerdt@math.tu-berlin.de (Paul Schwerdtner), matthias.voigt@fernuni.ch (Matthias Voigt)

rameters are optimized using gradient-based numerical optimization. There exist two implementations of this approach, HIFOO<sup>1</sup> (Burke et al., 2006) and hinfstruct<sup>2</sup> (Apkarian and Noll, 2006). Fixed-order  $\mathcal{H}_\infty$  synthesis leads to constraint nonsmooth and nonconvex optimization problems such that only locally optimal controllers can be computed. In contrast to that, full-order controllers are typically globally optimal<sup>3</sup>. However, both packages were applied successfully in industrial applications, see, e.g., Wang and Chen (2009); Gabarrou et al. (2010); Robu et al. (2010); Ravanbod and Noll (2012). In each iteration of the optimization, the  $\mathcal{H}_\infty$  norm of the closed-loop system must be evaluated and its stability must be checked. For systems with high state-space dimension, this can lead to prohibitively high computational costs.

To keep the computational costs manageable for large-scale systems, HIFOO is extended in Mitchell and Overton (2015) by using a new method for the  $\mathcal{H}_\infty$  norm computation of large-scale systems (Mitchell and Overton, 2016) and in Benner et al. (2018) by using a reduced-order approximation to the given large-scale plant. Recently, in Werner et al. (2022), controllers are computed using several reduced-order plants at different fidelity levels. To ensure stability, in the large-scale setting, iterative methods can be employed as in Benner et al. (2018) to compute the rightmost eigenvalues of the closed-loop system matrix. When iterative methods are used, technically, stability cannot be ensured, as the convergence to the rightmost eigenvalue of the closed-loop system matrix is not guaranteed. Moreover, in Benner et al. (2018) it is noted that the stability constraint in the large-scale  $\mathcal{H}_\infty$  control problem poses a particular challenge during optimization, which requires several restarts of the  $\mathcal{H}_\infty$  optimization in (Benner et al., 2018, Algorithm 2). Moreover, performing large-scale  $\mathcal{H}_\infty$  norm evaluations during controller synthesis as in Mitchell and Overton (2015) is reported to potentially lead to a premature halt of the optimization (Benner et al., 2018, Section 2).

In this article, by using the pH paradigm, we can use a different strategy to ensure stability of large-scale closed-loop systems based on the following well-known fact: The negative feedback interconnection of two pH systems (see Section 3) is again pH and thus Lyapunov stable. Therefore, we propose to use a pH controller to ensure Lyapunov stability of the closed-loop system directly from the model structure. In fact, since the pH structure can be encoded into our controller parameterization, we can use unconstrained optimization. To avoid computing the  $\mathcal{H}_\infty$  norm of the potentially large-scale closed-loop systems repeatedly, we use the sample-based optimization approach developed in Schwerdtner and Voigt (2020, 2021) for  $\mathcal{H}_\infty$ -

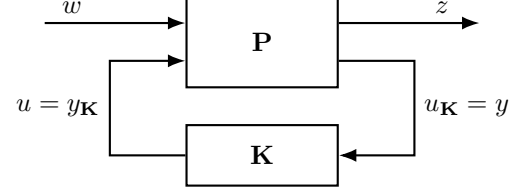


Figure 1: Closed-loop system obtained by coupling the plant  $\mathbf{P}$  with the controller  $\mathbf{K}$

inspired model order reduction. In this way, we may compute stabilizing controllers for pH systems that only require the evaluation of the transfer function of the given plant.

Our article is organized as follows. In the next section, we recall the fixed-order  $\mathcal{H}_\infty$  synthesis problem. After that, we briefly explain pH systems and the connections between pH and passive systems. In Section 5, we explain our approach and in Section 6 we provide a comparison to the other fixed-order  $\mathcal{H}_\infty$  synthesis methods.

## 2. $\mathcal{H}_\infty$ Controller Synthesis

The setup of the classical  $\mathcal{H}_\infty$  controller design problem consisting of a plant  $\mathbf{P}$  and a controller  $\mathbf{K}$  is illustrated in Figure 1. The plant is defined as

$$\mathbf{P} : \begin{bmatrix} \dot{x}(t) \\ z(t) \\ y(t) \end{bmatrix} = \begin{bmatrix} A & B_1 & B_2 \\ C_1 & D_{11} & D_{12} \\ C_2 & D_{21} & D_{22} \end{bmatrix} \begin{bmatrix} x(t) \\ w(t) \\ u(t) \end{bmatrix}$$

with  $A \in \mathbb{R}^{n \times n}$ ,  $B_j \in \mathbb{R}^{n \times m_j}$ ,  $C_i \in \mathbb{R}^{p_i \times n}$ , and  $D_{ij} \in \mathbb{R}^{p_i \times m_j}$  for  $i, j = 1, 2$ . For  $t \in [0, \infty)$ ,  $x$  denotes the *state*,  $u$  and  $w$  denote the *control* and *disturbance* input, respectively, whereas  $y$  and  $z$  denote the *measured* and *performance* output, respectively. A controller of order  $k$  is given by

$$\mathbf{K} : \begin{bmatrix} \dot{x}_K(t) \\ y_K(t) \end{bmatrix} = \begin{bmatrix} A_K & B_K \\ C_K & D_K \end{bmatrix} \begin{bmatrix} x_K(t) \\ u_K(t) \end{bmatrix}$$

with  $A_K \in \mathbb{R}^{k \times k}$ ,  $B_K \in \mathbb{R}^{k \times p_2}$ ,  $C_K \in \mathbb{R}^{m_2 \times k}$ , and  $D_K \in \mathbb{R}^{m_2 \times p_2}$ , and is coupled with the plant  $\mathbf{P}$  by the coupling conditions  $u_K(\cdot) = y(\cdot)$  and  $u(\cdot) = y_K(\cdot)$ .

The goal in  $\mathcal{H}_\infty$  synthesis is to tune the controller, i.e., to determine matrices  $A_K, B_K, C_K$ , and  $D_K$  such that the performance output is minimized in an appropriate norm for all admissible disturbance inputs. This can be quantified using the *transfer functions* of plant and controller, that are defined as follows

$$\begin{aligned} P(s) &:= \begin{bmatrix} P_{11}(s) & P_{12}(s) \\ P_{21}(s) & P_{22}(s) \end{bmatrix} \\ &:= \begin{bmatrix} C_1 \\ C_2 \end{bmatrix} (sI_n - A)^{-1} \begin{bmatrix} B_1 & B_2 \end{bmatrix} + \begin{bmatrix} D_{11} & D_{12} \\ D_{21} & D_{22} \end{bmatrix}, \\ K(s) &:= C_K (sI_k - A_K)^{-1} B_K + D_K. \end{aligned} \quad (1)$$

<sup>1</sup>available at <https://cs.nyu.edu/~overton/software/hifoo/>

<sup>2</sup>available in MATLAB's Robust Control Toolbox

<sup>3</sup>For numerical reasons, full-order controllers are often designed as suboptimal controllers but with near globally optimal performance.

If the interconnection between  $\mathbf{P}$  and  $\mathbf{K}$  is *well-posed*, i. e.,  $\begin{bmatrix} I_{m_2} & -D_{\mathbf{K}_*} \\ -D_{22} & I_{p_2} \end{bmatrix}$  is invertible, then the closed-loop transfer function exists and is given by the *lower linear fractional transformation* of  $P$  and  $K$  defined as

$$(P \star K)(s) := P_{11}(s) + P_{12}(s)K(s)(I_{p_2} - P_{22}(s)K(s))^{-1}P_{21}(s).$$

An optimal controller  $\mathbf{K}_* = (A_{\mathbf{K}_*}, B_{\mathbf{K}_*}, C_{\mathbf{K}_*}, D_{\mathbf{K}_*})$  of order  $k$  then satisfies

$$\begin{aligned} \mathbf{K}_* &= \arg \min_{(A_{\mathbf{K}}, B_{\mathbf{K}}, C_{\mathbf{K}}, D_{\mathbf{K}})} \|P \star K\|_{\mathcal{H}_\infty}, \\ \text{s. t. } \mathcal{A}(\mathbf{K}) &\text{ is asymptotically stable,} \end{aligned}$$

where  $K$  is as in (1), the  $\mathcal{H}_\infty$  norm of  $P \star K$  is defined as

$$\begin{aligned} \|P \star K\|_{\mathcal{H}_\infty} &:= \sup_{s \in \mathbb{C}, \operatorname{Re}(s) > 0} \|(P \star K)(s)\|_2 \\ &= \sup_{\omega \in \mathbb{R}} \|(P \star K)(i\omega)\|_2, \end{aligned}$$

and  $\mathcal{A}(\mathbf{K})$  is the closed-loop system matrix, defined as

$$\begin{bmatrix} A & 0 \\ 0 & A_{\mathbf{K}} \end{bmatrix} + \begin{bmatrix} B_2 & 0 \\ 0 & B_{\mathbf{K}} \end{bmatrix} \begin{bmatrix} I_{m_2} & -D_{\mathbf{K}} \\ -D_{22} & I_{p_2} \end{bmatrix}^{-1} \begin{bmatrix} 0 & C_{\mathbf{K}} \\ C_2 & 0 \end{bmatrix}. \quad (2)$$

This matrix (resp. the closed-loop system) is called *asymptotically stable*, if all its eigenvalues have strictly negative real part.

### 3. Port-Hamiltonian Systems

In this article, we consider plant models, for which the subsystem from controller input to measured output can be written as a pH system.

**Definition 1.** A linear, constant-coefficient dynamical system of the form

$$\begin{bmatrix} \dot{x}(t) \\ y(t) \end{bmatrix} = \begin{bmatrix} (J - R)Q & G - F \\ (G + F)^\top Q & S - N \end{bmatrix} \begin{bmatrix} x(t) \\ u(t) \end{bmatrix} \quad (3)$$

is called a port-Hamiltonian system, if the matrices  $J, R, Q \in \mathbb{R}^{n \times n}$ ,  $G, F \in \mathbb{R}^{n \times m}$ , and  $S, N \in \mathbb{R}^{m \times m}$  satisfy the following constraints:

- (i) The matrices  $J$  and  $N$  are skew-symmetric.
- (ii) The passivity matrix  $W := \begin{bmatrix} R & F \\ F^\top & S \end{bmatrix}$  is symmetric positive semi-definite.
- (iii)  $Q$  is symmetric positive definite.

The Hamiltonian (energy-storage) function  $\mathcal{H} : \mathbb{R}^n \rightarrow \mathbb{R}$  is then given by

$$\mathcal{H}(x) = \frac{1}{2} x^\top Q x. \quad (4)$$

In this way, the plants that we consider can be formulated as

$$\begin{bmatrix} \dot{x}(t) \\ z(t) \\ y(t) \end{bmatrix} = \begin{bmatrix} (J - R)Q & B_1 & G - F \\ C_1 & D_{11} & D_{12} \\ (G + F)^\top Q & D_{21} & S - N \end{bmatrix} \begin{bmatrix} x(t) \\ w(t) \\ u(t) \end{bmatrix}, \quad (5)$$

with matrices  $J, R, Q, G, F, S$ , and  $N$  that satisfy the constraints imposed in Definition 1.

Port-Hamiltonian systems are also *passive*. This follows from the fact that the Hamiltonian (4) of a pH system (3) is a so-called *storage function* as it fulfills the *dissipation inequality*

$$\mathcal{H}(x(t_1)) \leq \mathcal{H}(x(t_0)) + \int_{t_0}^{t_1} y(t)^\top u(t) dt$$

for each solution trajectory  $(u, x, y)$  of (3) and for each  $t_0, t_1 \geq 0$  with  $t_0 \leq t_1$ . The converse is also true under the assumption of minimality<sup>4</sup>, i. e., each minimal passive system can be realized as a pH system by suitable state-space transformations (Beattie et al., 2022, Cor. 2). For a detailed analysis of such realizations, see also Cherifi et al. (2022). In the next section, we use this fact to define an intuitive approach to passivity-based  $\mathcal{H}_\infty$  control.

It is a well-known fact that the negative feedback interconnection of two passive systems is again passive (see Khalil (2002, Theorem 6.1)) and thus *Lyapunov stable*, i. e., all eigenvalues of the corresponding closed-loop system matrix have nonpositive real part and the ones on the imaginary axis are semi-simple. In our setting, a *negative feedback interconnection* is a coupling of the plant and controller obtained from the modified coupling conditions  $u_{\mathbf{K}}(\cdot) = y(\cdot)$  and  $u(\cdot) = -y_{\mathbf{K}}(\cdot)$ . We use this coupling in the remainder of this article.

We restate the passive interconnection result for pH systems and provide a proof because our setup differs slightly from the literature.

**Proposition 1.** Consider a pH plant model (without the channels  $w$  and  $z$ )

$$\mathbf{P}_{\text{pH}} : \begin{bmatrix} \dot{x}(t) \\ y(t) \end{bmatrix} = \begin{bmatrix} (J - R)Q & G - F \\ (G + F)^\top Q & S - N \end{bmatrix} \begin{bmatrix} x(t) \\ u(t) \end{bmatrix},$$

that satisfies the conditions in Definition 1, and a pH controller

$$\mathbf{K}_{\text{pH}} : \begin{bmatrix} \dot{x}_{\mathbf{K}}(t) \\ y_{\mathbf{K}}(t) \end{bmatrix} = \begin{bmatrix} (J_{\mathbf{K}} - R_{\mathbf{K}})Q_{\mathbf{K}} & G_{\mathbf{K}} - F_{\mathbf{K}} \\ (G_{\mathbf{K}} + F_{\mathbf{K}})^\top Q_{\mathbf{K}} & S_{\mathbf{K}} - N_{\mathbf{K}} \end{bmatrix} \begin{bmatrix} x_{\mathbf{K}}(t) \\ u_{\mathbf{K}}(t) \end{bmatrix},$$

that also satisfies the conditions in Definition 1. Then the negative feedback interconnection of  $\mathbf{P}_{\text{pH}}$  with  $\mathbf{K}_{\text{pH}}$  resulting from the coupling conditions  $u_{\mathbf{K}}(\cdot) = y(\cdot)$  and  $u(\cdot) = -y_{\mathbf{K}}(\cdot)$  results in a Lyapunov stable closed-loop system.

<sup>4</sup>A system is called minimal if it is controllable and observable; see Zhou et al. (1996)

*Proof.* The closed-loop matrix of the negative feedback interconnection of  $\mathbf{P}_{\text{pH}}$  and  $\mathbf{K}_{\text{pH}}$  is given by

$$\begin{bmatrix} (J-R)Q & 0 \\ 0 & (J_{\mathbf{K}} - R_{\mathbf{K}})Q_{\mathbf{K}} \end{bmatrix} + \begin{bmatrix} G-F & 0 \\ 0 & -G_{\mathbf{K}} + F_{\mathbf{K}} \end{bmatrix} \cdot \begin{bmatrix} I_m & S_{\mathbf{K}} - N_{\mathbf{K}} \\ -S + N & I_m \end{bmatrix}^{-1} \begin{bmatrix} 0 & (G_{\mathbf{K}} + F_{\mathbf{K}})^{\top} Q_{\mathbf{K}} \\ (G+F)^{\top} Q & 0 \end{bmatrix}.$$

Note the two additional minus signs compared to (2) that are due to the negative interconnection of  $\mathbf{P}_{\text{pH}}$  and  $\mathbf{K}_{\text{pH}}$ . This matrix has the structure of a Schur complement. By reverting the Schur complement and some additional permutations and scalings, it can be seen that this matrix has the same eigenvalues as the regular index-one matrix pencil (as defined in Kunkel and Mehrmann (2006, Chapter 2))

$$\begin{bmatrix} sI_n - (J-R)Q & 0 & -G+F & 0 \\ 0 & sI_k - (J_{\mathbf{K}} - R_{\mathbf{K}})Q_{\mathbf{K}} & 0 & -G_{\mathbf{K}} + F_{\mathbf{K}} \\ (G+F)^{\top} Q & 0 & S-N & I_m \\ 0 & (G_{\mathbf{K}} + F_{\mathbf{K}})^{\top} Q_{\mathbf{K}} & -I_m & S_{\mathbf{K}} - N_{\mathbf{K}} \end{bmatrix} \quad (6)$$

except for  $2m$  additional eigenvalues at infinity. This pencil can be written as  $s\mathcal{E} - (\mathcal{J} - \mathcal{R})\mathcal{Q}$ , where  $\mathcal{E}^{\top} \mathcal{Q} \succeq 0$  with  $\mathcal{Q} = \text{diag}(Q, Q_{\mathbf{K}}, I_m, I_m) \succ 0$ ,  $\mathcal{J} = -\mathcal{J}^{\top}$ , and  $\mathcal{R} \succeq 0$ .<sup>5</sup> Hence, it is a dissipative Hamiltonian pencil. Since the pencil  $s\mathcal{E} - \mathcal{Q}$  is regular as well, the assertion follows from Mehl et al. (2021, Thm. 2).  $\square$

**Remark 1.** Proposition 1 only shows that the negative feedback interconnection of the plant and the controller results in a Lyapunov stable closed-loop system. However, the closed-loop system matrix may still have undesired eigenvalues on the imaginary axis. For the unstructured problem, there are conditions that guarantee the existence of an asymptotically stabilizing full-order controller. However, for fixed-order control, these conditions fail to be valid, see, e.g., Geromel et al. (1998). Throughout our paper we assume that an asymptotically stabilizing pH controller exists. An obvious sufficient condition that is also often satisfied in practice is the asymptotic stability of  $(J-R)Q$ ; this has also been assumed in the recent work Breiten and Karsai (2022).

#### 4. Passivity Enforcement

The close connection between passive and pH controllers (see Theorem 1 below) permits the computation of a pH controller by means of an alternative indirect approach: first a general controller is computed using either of the established fixed-order  $\mathcal{H}_{\infty}$  synthesis methods HIFOO or hinfstruct and then, in a post-processing step, a passivity-check determines, whether the controller

is already passive and can be directly transformed to pH form or if another passivity enforcement step must first be applied. This post-processing approach is typically applied successfully in passivity-based system identification; see e.g. Gustavsen and Semlyen (2001); Grivet-Talocia (2004); Oliveira et al. (2016).

If a controller  $\mathbf{K}$  is passive, then its transfer function  $K$  is *positive real* as in the following definition.

**Definition 2.** A proper real-rational transfer function  $K$  is called *positive real*, if (i) all poles of  $K$  have non-positive real part, (ii) the matrix-valued Popov function  $\Phi(s) := K(-s)^{\top} + K(s)$  attains positive semi-definite values for all  $s \in i\mathbb{R}$ , which are not poles of  $K$ , and (iii) for any purely imaginary pole  $i\omega$  of  $K$  we have that the residue matrix  $\lim_{s \rightarrow i\omega} (s - i\omega)K(s)$  is positive semi-definite.

The equivalences between passivity, positive-real transfer functions, and a possible pH formulation are summarized in the following theorem. A proof can be found in Beattie et al. (2018).

**Theorem 1.** Assume that a controller  $\mathbf{K}$  of order  $k$  is minimal and Lyapunov stable. Then the following statements are equivalent:

- (i)  $\mathbf{K}$  is passive.
- (ii) The controller transfer function  $K$  is positive real as defined in Definition 2.
- (iii)  $\mathbf{K}$  can be written as pH controller.
- (iv) There exists a symmetric positive definite matrix  $X \in \mathbb{R}^{k \times k}$  satisfying the Kalman-Yakubovich-Popov (KYP) inequality

$$\begin{bmatrix} -A_{\mathbf{K}}^{\top} X - X A_{\mathbf{K}} & C_{\mathbf{K}}^{\top} - X B_{\mathbf{K}} \\ C_{\mathbf{K}} - B_{\mathbf{K}}^{\top} X & D_{\mathbf{K}} + D_{\mathbf{K}}^{\top} \end{bmatrix} \succeq 0.$$

Checking  $\mathbf{K}$  for passivity is straight-forward. We can simply check if the KYP inequality can be satisfied using either an ARE or LMI solver. For passivity enforcement, there exist several strategies, such as Grivet-Talocia (2004); Coelho et al. (2004); Gillis and Sharma (2018). An extensive discussion on well-established passivity enforcement methods is presented in Grivet-Talocia and Gustavsen (2015, Chapter 10). In our numerical experiments, we use the LMI-based method for passivity enforcement presented in Coelho et al. (2004) due to its moderate computational cost for small controller orders and its straight-forward implementation. It is based on computing a minimally perturbed controller output  $\hat{C}_{\mathbf{K}} := C_{\mathbf{K}} + \Xi L_c$ , where  $L_c$  is the Cholesky factor of the *controllability Gramian*<sup>6</sup> of  $\mathbf{K}$ , such that the

<sup>5</sup>The notation  $X \succ 0$  ( $X \succeq 0$ ) denotes the positive (semi-) definiteness of a real symmetric matrix  $X$ .

<sup>6</sup>The controllability gramian of  $\mathbf{K}$  can be computed as solution  $P_c$  to the Lyapunov equation  $A_{\mathbf{K}} P_c + P_c A_{\mathbf{K}}^{\top} + B_{\mathbf{K}} B_{\mathbf{K}}^{\top} = 0$ .



perturbed KYP inequality

$$\mathcal{W}(X, \Xi) := \begin{bmatrix} -A_{\mathbf{K}}^T X - X A_{\mathbf{K}} & \tilde{C}_{\mathbf{K}}^T - X B_{\mathbf{K}} \\ \tilde{C}_{\mathbf{K}} - B_{\mathbf{K}}^T X & D_{\mathbf{K}} + D_{\mathbf{K}}^T \end{bmatrix} \succeq 0.$$

admits a solution. The convex optimization problem that computes a minimally perturbed controller is given by

$$\min \|\Xi\|_F \quad \text{s. t.} \quad \mathcal{W}(X, \Xi) \succeq 0, \quad X \succ 0, \quad (7)$$

which is a standard LMI problem that we solve in our numerical experiments using the method presented in [O'Donoghue et al. \(2016\)](#).

The main problem with this passivity enforcement method is emphasized in our numerical experiments: The generic controllers computed using either `hinfstruct` or `HIFOO` often require a large perturbation to be made passive, which deteriorates the  $\mathcal{H}_\infty$  performance. Moreover, passivity enforcement methods focus on minimally changing the transfer function of the controller but naturally do not take the  $\mathcal{H}_\infty$  performance of the resulting closed-loop transfer function into account. Instead, the method we present in the following section computes passive controllers that aim directly at minimizing the  $\mathcal{H}_\infty$  norm of the closed-loop transfer function.

## 5. Our Approach: Structured Optimization-Based Synthesis

Our approach for pH  $\mathcal{H}_\infty$  synthesis is an adaptation of the model order reduction method developed in [Schwerdtner and Voigt \(2020, 2021\)](#). Following a similar strategy, we only make use of samples of the closed-loop transfer function to avoid the computation of the  $\mathcal{H}_\infty$  norm of  $P \star K$  and impose the pH structure of the controller directly in our parameterization such that no constraints have to be enforced during optimization. The parameterization is described in Lemma 1 and our optimization method is given in detail in Algorithm 1. We call our method SOBSYN (Structured Optimization-Based SYNthesis).

**Lemma 1.** [[Schwerdtner and Voigt \(2020\)](#)] *Let  $\theta \in \mathbb{R}^{n_\theta}$  be a parameter vector that is partitioned as  $\theta = [\theta_J^T, \theta_W^T, \theta_G^T, \theta_Q^T, \theta_N^T]^T$ , with  $\theta_J \in \mathbb{R}^{k(k-1)/2}$ ,  $\theta_W \in \mathbb{R}^{(k+p_2)(k+p_2+1)/2}$ ,  $\theta_Q \in \mathbb{R}^{k(k+1)/2}$ ,  $\theta_G \in \mathbb{R}^{kp_2}$ , and  $\theta_N \in \mathbb{R}^{p_2(p_2-1)}$ . We define the matrices*

$$J(\theta) = \text{vtsu}(\theta_J)^T - \text{vtsu}(\theta_J), \quad (8a)$$

$$W(\theta) = \text{vtu}(\theta_W)^T \text{vtu}(\theta_W), \quad (8b)$$

$$Q(\theta) = \text{vtu}(\theta_Q)^T \text{vtu}(\theta_Q), \quad (8c)$$

$$G(\theta) = \text{vtf}_{k, m_2}(\theta_G), \quad (8d)$$

$$N(\theta) = \text{vtsu}(\theta_N)^T - \text{vtsu}(\theta_N), \quad (8e)$$

where the functions  $\text{vtu} : \mathbb{R}^{k(k+1)/2} \rightarrow \mathbb{R}^{k \times k}$  [or  $\text{vtsu} : \mathbb{R}^{(k+p_2)(k+p_2+1)/2} \rightarrow \mathbb{R}^{(k+p_2) \times (k+p_2)}$ ] (resp.

$\text{vtsu} : \mathbb{R}^{k(k-1)} \rightarrow \mathbb{R}^{k \times k}$ ) map vectors to upper (resp. strictly upper) triangular matrices, while the function  $\text{vtf} : \mathbb{R}^{k \cdot m_2} \rightarrow \mathbb{R}^{k \times m_2}$  reshapes a vector of length  $km_2$  to a  $k \times m_2$  matrix. Then, if  $\theta \in \mathbb{R}^{n_\theta}$  is such that  $Q(\theta) \succ 0$ , a pH controller of order  $k$  can be defined as

$$\begin{bmatrix} \dot{x}_{\mathbf{K}}(t) \\ y_{\mathbf{K}}(t) \end{bmatrix} = \begin{bmatrix} (J_{\mathbf{K}}(\theta) - R_{\mathbf{K}}(\theta))Q_{\mathbf{K}}(\theta) & G_{\mathbf{K}}(\theta) - F_{\mathbf{K}}(\theta) \\ (G_{\mathbf{K}}(\theta) + F_{\mathbf{K}}(\theta))^T Q_{\mathbf{K}}(\theta) & S_{\mathbf{K}}(\theta) - N_{\mathbf{K}}(\theta) \end{bmatrix} \begin{bmatrix} x_{\mathbf{K}}(t) \\ u_{\mathbf{K}}(t) \end{bmatrix}, \quad (9)$$

where  $R(\theta)$ ,  $F(\theta)$ , and  $S(\theta)$  are extracted from  $W(\theta)$  as

$$R(\theta) := [I_k \quad 0] W(\theta) [I_k \quad 0]^T,$$

$$F(\theta) := [I_k \quad 0] W(\theta) [0 \quad I_{m_2}]^T,$$

$$S(\theta) := [0 \quad I_{m_2}] W(\theta) [0 \quad I_{m_2}]^T.$$

Conversely, to each pH controller  $\mathbf{K}_{\text{pH}}$  with  $k$  states and  $m_2$  inputs and outputs, a vector  $\theta \in \mathbb{R}^{n_\theta}$  can be defined such that  $\mathbf{K}_{\text{pH}} = \mathbf{K}_{\text{pH}}(\theta)$ .

This parameterization is well-suited for low-order pH systems. For higher orders, the number of parameters can be excessive. A generalization of this parameterization to pH systems with algebraic constraints is developed in [Moser et al. \(2022\)](#).

We can now define the optimization problem. If  $K(\theta)(\cdot)$  denotes the transfer function of  $\mathbf{K}_{\text{pH}}(\theta)$ , our objective function is defined as

$$\mathcal{L}(\gamma, P, K(\theta), \mathcal{S}) := \frac{1}{\gamma} \sum_{s_i \in \mathcal{S}} \sum_{j=1}^{\min(m_1, p_1)} \left( [\sigma_j((P \star K(\theta))(s_i)) - \gamma]_+ \right)^2, \quad (10)$$

where

$$[\cdot]_+ : \mathbb{R} \rightarrow \overline{\mathbb{R}}^+, \quad x \mapsto \begin{cases} x & \text{if } x \geq 0, \\ 0 & \text{if } x < 0, \end{cases}$$

$\mathcal{S} \subseteq i\mathbb{R}$  is the set of sample points at which the closed-loop transfer function is evaluated, and  $\sigma_j$  denotes the  $j$ -th singular value of its matrix argument. In Algorithm 1, we minimize  $\mathcal{L}$  w. r. t.  $\theta$  for decreasing values of the threshold value  $\gamma$  to attain a controller  $\mathbf{K}_{\text{pH}}(\theta)$  that leads to a small  $\mathcal{H}_\infty$  norm of the closed-loop transfer function. In [Schwerdtner and Voigt \(2020, Remark 3.1\)](#) we explain the benefits resulting from a minimization of  $\mathcal{L}$  compared to a direct minimization of the  $\mathcal{H}_\infty$  norm in the context of model order reduction. The arguments carry over directly to  $\mathcal{H}_\infty$  synthesis.

1. The repeated computation of the  $\mathcal{H}_\infty$  norm of the (potentially large-scale) closed-loop transfer function is computationally demanding despite novel approaches for the  $\mathcal{H}_\infty$  norm computation of large-scale transfer functions ([Aliyev et al., 2017](#); [Guglielmi et al., 2013](#); [Mitchell and Overton, 2016](#)). In contrast to that, an evaluation of  $\mathcal{L}$  can be carried out even for large-scale plants and the plant transfer function evaluations can be cached for subsequent evaluations of  $\mathcal{L}$ .

---

**Algorithm 1:** SOBSYN

---

**Input** : Plant transfer function  $P$ , initial controller transfer function  $K(\theta_0)$  with parameter  $\theta_0 \in \mathbb{R}^{n_\theta}$ , initial sample point set  $\mathcal{S} \subset \mathbb{i}\mathbb{R}$ , upper bound  $\gamma_u > 0$ , bisection tolerance  $\varepsilon_1 > 0$ , termination tolerance  $\varepsilon_2 > 0$

**Output:**  $\mathcal{H}_\infty$  controller of order  $k$

```
1 Set  $j := 0$  and  $\gamma_l := 0$ .
2 while  $(\gamma_u - \gamma_l)/(\gamma_u + \gamma_l) > \varepsilon_1$  do
3   Set  $\gamma := (\gamma_u + \gamma_l)/2$ .
4   Update the sample point set  $\mathcal{S}$ 
   using Schwerdtner and Voigt \(2021, Alg. 3.1\).
5   Solve the minimization problem
    $\alpha := \min_{\theta \in \mathbb{R}^{n_\theta}} \mathcal{L}(\gamma, P, K(\theta), \mathcal{S})$  with minimizer
    $\theta_{j+1} \in \mathbb{R}^{n_\theta}$ , initialized at  $\theta_j$ .
6   if  $\alpha > \varepsilon_2$  then
7     Set  $\gamma_l := \gamma$ .
8   else
9     Set  $\gamma_u := \gamma$ .
10  end
11  Set  $j := j + 1$ .
12 end
13 Construct the controller with  $\theta_j$  as in Lemma 1.
```

---

2. The  $\mathcal{H}_\infty$  norm depends only continuously on the controller parameters but is not differentiable in general, which requires the use of nonsmooth optimization solvers. This poses additional theoretical and computational challenges. In contrast,  $\mathcal{L}$  is differentiable with respect to the controller parameters; see [Schwerdtner and Voigt \(2020, Proposition 3.1\)](#).
3. The gradient of the  $\mathcal{H}_\infty$  norm (if it exists) contains only limited information for an overall good descent direction because it only considers the closed-loop transfer function at a single point. In contrast,  $\mathcal{L}$  takes into account  $P \star K(\theta)$  at all points  $s_i$ , where a singular value of  $P \star K(\theta)$  is larger than  $\gamma$ .

Since  $\mathcal{L}$  only takes into account the closed-loop transfer function at sample points  $s_i$ , it is important to choose a suitable sample point set  $\mathcal{S}$ . If the sample points are distributed such that some local maxima of  $\|(P \star K(\theta))(i \cdot)\|_2$  are missed entirely, then a minimization of  $\mathcal{L}$  does not lead to a good  $\mathcal{H}_\infty$  performance. However, an abundance of sample points leads to unnecessary computational effort. Therefore, in [Schwerdtner and Voigt \(2021\)](#), an adaptive sampling strategy introduced in [Apkarian and Noll \(2018\)](#) is adapted for use in combination with  $\mathcal{L}$ . The method is motivated and described in detail in [Schwerdtner and Voigt \(2021, Algorithm 1\)](#). It can be used directly in our proposed  $\mathcal{H}_\infty$  synthesis algorithm, which is described in [Algorithm 1](#).

SOBSYN is based on a bisection over  $\gamma$ . After an update of the sample set  $\mathcal{S}$  in each iteration, we compute a minimizer for  $\mathcal{L}$  at the current  $\gamma$ -level using the BFGS-based optimization solver implemented in [Mogensen and Riseth \(2018\)](#). If the minimum  $\alpha$  is lower than  $\varepsilon_2$ , the solver has managed to reduce all singular values of the closed-loop transfer function evaluated at all sample points below the current  $\gamma$ -level up to the *termination tolerance*  $\varepsilon_2$ . In this case, we reduce the upper bound to  $\gamma_u := \gamma$ ; otherwise, we increase the lower bound to  $\gamma_l := \gamma$ . We terminate the bisection, when the relative difference between  $\gamma_u$  and  $\gamma_l$  is lower than the *bisection tolerance*  $\varepsilon_1$ .

## 6. Numerical Experiments

In our first experiment, we demonstrate the effectiveness of our method on the passive systems within the *COMPlib* benchmark collection ([Leibfritz, 2004](#)), which is often used to benchmark  $\mathcal{H}_\infty$  controller synthesis algorithms; see, e.g. [Apkarian and Noll \(2006\)](#); [Burke et al. \(2006\)](#). We only use plants, which can be rewritten as in (5), as our algorithm only applies to these cases. We compare our method to the general purpose fixed-order  $\mathcal{H}_\infty$  synthesis methods HIF00 and **hinfstruct**.

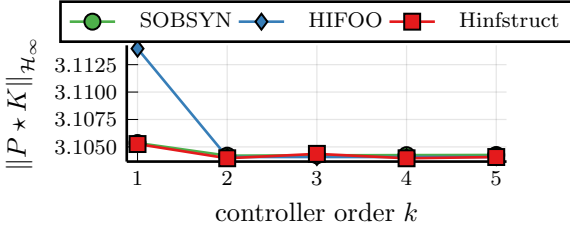
The structure of this experiment is as follows. For each benchmark plant, we apply HIF00, **hinfstruct**, and our method to generate a controller for controller orders  $k = 1, \dots, 5$ . After a comparison of the  $\mathcal{H}_\infty$  performance of all controllers, we solve (7) to compute passive approximations to the controllers computed with HIF00 and **hinfstruct** and re-evaluate the  $\mathcal{H}_\infty$  performance for the passive controllers. We only report a subset of the conducted experiments that is representative for our overall observations.<sup>7</sup>

In [Figure 2](#), we plot the  $\mathcal{H}_\infty$  performance of the controllers computed with our method and with HIF00 and **hinfstruct** for different models and controller orders. There are some differences in the  $\mathcal{H}_\infty$  performances across the models and controller orders but no method is systematically leading to worse results. This is despite the fact that SOBSYN is restricted to compute pH controllers only. Just for the DLR1 model, our method leads to slightly worse controllers than the other two methods for the orders  $k = 2, \dots, 5$ .

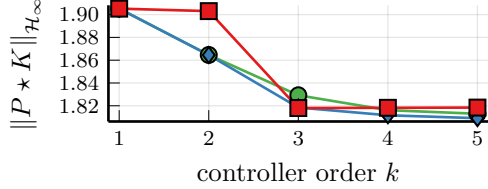
In [Figure 4](#), we compare the  $\mathcal{H}_\infty$  performance of SOBSYN to the  $\mathcal{H}_\infty$  performance of the HIF00 and **hinfstruct** controllers after the passivation step is applied. For EB1, the HIF00 and **hinfstruct** controllers are already mostly passive such that only for  $r \in \{3, 5\}$ , the  $\mathcal{H}_\infty$  performance is slightly worse for **hinfstruct**. In EB6, we can observe the potentially damaging behavior of the passivation step to the  $\mathcal{H}_\infty$  performance. Here the  $\mathcal{H}_\infty$  norm of the closed-loop transfer function increases by

---

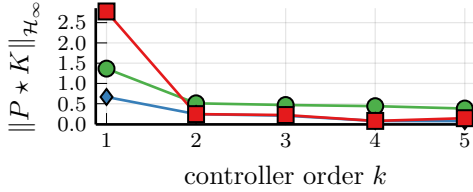
<sup>7</sup>The remaining experimental results are available at [zenodo.org/record/7049952](https://zenodo.org/record/7049952).



(a) EB1 model

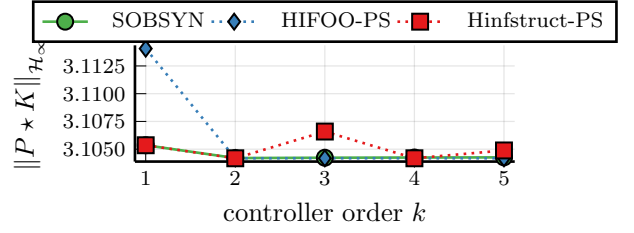


(b) EB6 model

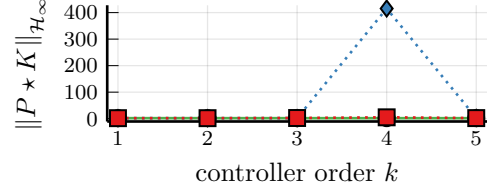


(c) DLR1 model

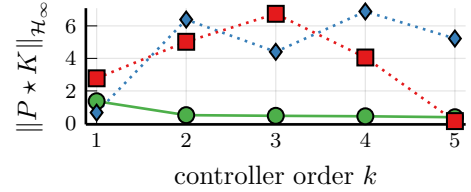
Figure 2:  $\mathcal{H}_\infty$  performance for general controllers



(a) EB1 model



(b) EB6 model



(c) DLR1 model

Figure 4:  $\mathcal{H}_\infty$  performance for passive controllers

more than two orders of magnitudes after the passivation. In Figure 4 (c) we can observe, that for the DLR1 model, most HIFOO and **hinfstruct** controllers are not passive such that the passivation step deteriorates their  $\mathcal{H}_\infty$  performance significantly. In Figure 3, we show the eigenvalues of the Popov function evaluated on the imaginary axis for one of the controllers computed with HIFOO. The figure reveals that some the eigenvalues are significantly below zero, which emphasizes that passivity enforcement often has to change the general purpose controllers drastically to make them passive.

In our second experiment we use a scalable mass-spring-damper (MSD) system in port-Hamiltonian form to evaluate the impact of the plant order on the runtime of our method. The model is derived in Gugercin et al. (2012)

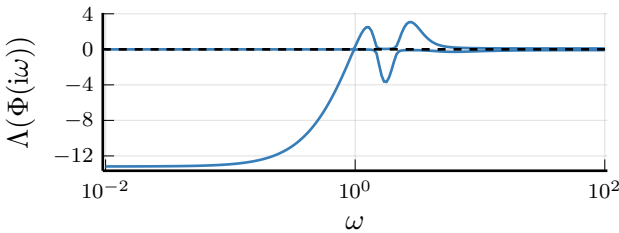


Figure 3: Eigenvalues of the Popov function of the order 5 controller for the DLR1 model computed with HIFOO

and the corresponding  $\mathcal{H}_\infty$  control problem is described in the collection of pH benchmark systems.<sup>8</sup> The state-space dimension of the model can be scaled by changing the number of masses that are included in the MSD chain. The runtimes and  $\mathcal{H}_\infty$  performances for plant orders from 10 to 2000 and controller orders 1, 5, and 10 are reported in Table 1. It can be observed, that while the runtimes increase significantly for HIFOO and **hinfstruct** as the plant dimension  $n$  is increased (**hinfstruct** takes almost 50 hours to compute a controller for the plant with state dimension 2000), the runtime of SOBSYN is less affected from an increase of  $n$ . However, we can observe that the controller dimension affects the runtime, which is well-aligned with our previous findings (Schwerdtner and Voigt, 2021, 2020). In general, the runtime of SOBSYN stays well under an hour for all plant and controller orders. The overall best  $\mathcal{H}_\infty$  performance is provided by **hinfstruct** across the different plant and controller orders. HIFOO often leads to a slightly worse performance than **hinfstruct**. In contrast to the previous experiment, SOBSYN has the worst  $\mathcal{H}_\infty$  performance for low plant orders (up to 50) but for medium to large plant orders, SOBSYN achieves an  $\mathcal{H}_\infty$  performance, that ranks between **hinfstruct** and HIFOO. When comparing the  $\mathcal{H}_\infty$  performance of SOBSYN to the other two methods, it is important to note that the other

<sup>8</sup>available at <https://perma.cc/297G-NFUJ>

they only result in one passive controller in this second experiment (for HIFOO at  $n = 1000$  and  $k = 5$ ). We can again expect a worse performance after a passivation step is applied as demonstrated in the previous experiment. However, this also emphasizes the fact that for certain plants, general controllers can lead to a better  $\mathcal{H}_\infty$  performance than controllers that are restricted to be passive.

## 7. Conclusion

We have presented SOBSYN, a new algorithm for the computation of fixed-order pH controllers for pH plants that aim at a low  $\mathcal{H}_\infty$  norm of the resulting closed-loop system. The main features of our algorithm in comparison to other fixed-order  $\mathcal{H}_\infty$  methods are the sample-based objective function and the passivity-based stability guarantee. Both features facilitate the application of our method to pH plants with high state-space dimension. Moreover, the sample-based nature of the objective function and its passivity-based stability also enables the computation of  $\mathcal{H}_\infty$  controllers in a purely data-driven way. Therefore, we can compute passive  $\mathcal{H}_\infty$  controllers for passive plants even if no access to the plant system matrices is possible but only transfer function evaluations are available.

While our adaptive sampling procedure works well in our experiments (and also in the much larger set of previously conducted model order reduction experiments), it is still possible that sharp peaks in the spectral norm of the closed-loop frequency response are missed. Therefore, it is recommended to validate the final controller performance. For small or medium systems, this can be done quickly using well-established  $\mathcal{H}_\infty$  norm computation. For large-scale systems, an  $\mathcal{H}_\infty$  certificate developed in Schwerdtner et al. (2020) may be used. We currently investigate the incorporation of such a certificate into the sampling stage of our method.

## Acknowledgements

We thank Volker Mehrmann for his helpful comments on an earlier version of this manuscript.

## References

Aliyev, N., Benner, P., Mengi, E., Schwerdtner, P., Voigt, M., 2017. Large-scale computation of  $\mathcal{L}_\infty$ -norms by a greedy subspace method. *SIAM J. Matrix Anal. Appl.* 38, 1496–1516.

Anderson, B.D.O., Liu, Y., 1989. Controller reduction: concepts and approaches. *IEEE Trans. Automat. Control* 34, 802–812.

Apkarian, P., Noll, D., 2006. Nonsmooth  $H_\infty$  synthesis. *IEEE Trans. Automat. Control* 51, 71–86.

Apkarian, P., Noll, D., 2018. Structured  $H_\infty$ -control of infinite-dimensional systems. *Internat. J. Robust Nonlinear Control* 28, 3212–3238.

Beattie, C., Mehrmann, V., Xu, H., 2022. Port-Hamiltonian Realizations of linear time invariant systems. *arXiv preprint arXiv:2201.05355*. Available at <https://arxiv.org/abs/2201.05355>.

Beattie, C., Mehrmann, V., Xu, H., Zwart, H., 2018. Linear port-Hamiltonian descriptor systems. *Math. Control Signals Systems* 30, 17.

Benner, P., Byers, R., Losse, P., Mehrmann, V., Xu, H., 2011. Robust formulas for optimal  $H_\infty$  controllers. *Automatica J. IFAC* 47, 2639–2646.

Benner, P., Byers, R., Mehrmann, V., Xu, H., 2002. Numerical computation of deflating subspaces of skew-Hamiltonian/Hamiltonian pencils. *SIAM J. Matrix Anal. Appl.* 24, 165–190.

Benner, P., Heiland, J., Werner, S.W.R., 2022. Robust output-feedback stabilization for incompressible flows using low-dimensional  $H_\infty$ -controllers. *Comput. Optim. Appl.* 82, 225–249.

Benner, P., Mitchell, T., Overton, M.L., 2018. Low-order control design using a reduced-order model with a stability constraint on the full-order model, in: *Proc. 2018 IEEE Conference on Decision and Control (CDC)*, Miami, FL, USA. pp. 3000–3005.

Breiten, T., Karsai, A., 2022. Structure Preserving  $H_\infty$  Control for Port-Hamiltonian Systems. *arXiv preprint arXiv:2206.08706*. Available at <https://arxiv.org/abs/2206.08706>.

Burke, J.V., Henrion, D., Lewis, A.S., Overton, M.L., 2006. HIFOO — a MATLAB package for fixed-order controller design and  $H_\infty$  optimization. *IFAC Proc. Vol.* 39, 339–344.

Cherifi, K., Gernandt, H., Hinsen, D., 2022. The difference between port-Hamiltonian, passive and positive real descriptor systems. Available at <https://arxiv.org/abs/2204.04990>.

Coelho, C.P., Phillips, J., Silveira, L.M., 2004. A convex programming approach for generating guaranteed passive approximations to tabulated frequency-data. *IEEE Trans. Computer-Aided Des. Integr. Circuits Systems* 23, 293–301.

Francis, B.A., 1987. *A Course in  $H_\infty$  Control Theory*. volume 88 of *Lect. Notes Control Inf. Sci.* Springer, Berlin, Heidelberg.

Gabarró, M., Alazard, D., Noll, D., 2010. Structured flight control law design using non-smooth optimization. *IFAC Proc. Vol.* 43, 536–541.

Geromel, J.C., de Souza, C.C., Skelton, R.E., 1998. Static output feedback controllers: Stability and convexity. *IEEE Trans. Automat. Control* 43, 120–125.

Gillis, N., Sharma, P., 2018. Finding the nearest positive-real system. *SIAM Journal on Numerical Analysis* 56, 1022–1047. doi:[10.1137/17M1137176](https://doi.org/10.1137/17M1137176).

Grivet-Talocia, S., 2004. Passivity enforcement via perturbation of Hamiltonian matrices. *IEEE Trans. Circuits Syst. I. Regul. Pap.* 51, 1755–1769.

Grivet-Talocia, S., Gustavsen, B., 2015. *Passive Macromodeling*. Wiley Ser. Microwave Optical Engrg., Wiley, Nashville, TN.

Gugercin, S., Polyuga, R.V., Beattie, C., van der Schaft, A., 2012. Structure-preserving tangential interpolation for model reduction of port-Hamiltonian systems. *Automatica J. IFAC* 48, 1963–1974.

Guglielmi, N., Gürbüzbalaban, M., Overton, M.L., 2013. Fast approximation of the  $H_\infty$  norm via optimization over spectral value sets. *SIAM J. Matrix Anal. Appl.* 34, 709–737.

Gustavsen, B., Semlyen, A., 2001. Enforcing passivity for admittance matrices approximated by rational functions. *IEEE Trans. Power Syst.* 16, 97–104.

Hauschild, S.A., Marheineke, N., Mehrmann, V., Mohring, J., Badlyan, A.M., Rein, M., Schmidt, M., 2020. Port-Hamiltonian modeling of district heating networks, in: Reis, T., Grundel, S., Schöps, S. (Eds.), *Progress in Differential-Algebraic Equations II*. Springer, Cham. *Differ.-Algebr. Equ. Forum*, pp. 333–355.

Khalil, H.K., 2002. *Nonlinear Systems*. Prentice-Hall, Upper Saddle River, NJ.

Kunkel, P., Mehrmann, V., 2006. *Differential-Algebraic Equations: Analysis and Numerical Solution*. EMS Publishing House, Zürich.

Leibfritz, F., 2004. *COMPlib: CONstrained Matrix-optimization Problem library* — a collection of test examples for nonlinear semidefinite programs, control system design and related problems. Available at [http://www.friedemann-leibfritz.de/COMPlib\\_Data/COMPlib\\_Main\\_Paper](http://www.friedemann-leibfritz.de/COMPlib_Data/COMPlib_Main_Paper)

Mehl, C., Mehrmann, V., Wojtylak, M., 2021. Distance problems for dissipative Hamiltonian systems and related matrix polynomials. *Linear Algebra Appl.* 623, 335–366.



Table 1:  $\mathcal{H}_\infty$  performance and runtimes of HIF00, hinfstruct, and SOBSYN for the MSD plants at different state dimensions. The runtimes are given in seconds. For  $n = 2000$ , HIF00 failed for all controller orders. We use an Intel® Core™ i9-9900K CPU at 3.60 GHz with 32 GB of RAM.

$n$		HIF00			hinfstruct			SOBSYN		
		$k = 1$	$k = 5$	$k = 10$	$k = 1$	$k = 5$	$k = 10$	$k = 1$	$k = 5$	$k = 10$
10	$\mathcal{H}_\infty$ -norm	5.2e−01	3.8e−01	4.4e−01	4.3e−01	4.2e−01	5.1e−01	4.9e−01	4.6e−01	4.6e−01
	runtime	3.8e+01	1.8e+01	1.2e+01	7.5e+00	1.0e+00	7.4e−01	8.3e+00	1.8e+02	1.2e+03
20	$\mathcal{H}_\infty$ -norm	4.6e−01	3.0e−01	3.7e−01	3.4e−01	2.9e−01	3.2e−01	4.0e−01	3.9e−01	3.8e−01
	runtime	5.9e+01	3.3e+01	1.4e+01	7.0e−01	2.4e+00	1.6e+00	2.6e+01	1.2e+02	7.2e+02
50	$\mathcal{H}_\infty$ -norm	3.2e−01	3.8e−01	3.7e−01	3.3e−01	3.1e−01	3.1e−01	3.9e−01	3.8e−01	3.8e−01
	runtime	8.5e+01	9.3e+02	3.8e+01	1.7e+00	2.7e+00	4.3e+00	2.0e+01	2.0e+02	1.0e+03
100	$\mathcal{H}_\infty$ -norm	4.5e−01	3.9e−01	3.5e−01	3.2e−01	3.1e−01	3.0e−01	3.9e−01	3.8e−01	3.8e−01
	runtime	1.2e+03	3.7e+03	1.7e+02	1.4e+01	1.4e+01	1.4e+01	1.8e+01	4.4e+02	9.3e+02
500	$\mathcal{H}_\infty$ -norm	4.3e−01	3.9e−01	3.5e−01	3.2e−01	3.1e−01	3.0e−01	3.9e−01	3.8e−01	3.8e−01
	runtime	5.2e+03	6.4e+03	7.9e+03	9.1e+02	7.8e+02	9.7e+02	1.6e+01	4.6e+02	9.7e+02
1000	$\mathcal{H}_\infty$ -norm	4.7e−01	4.0e−01	4.0e−01	3.2e−01	3.1e−01	3.1e−01	3.9e−01	3.8e−01	3.8e−01
	runtime	7.3e+03	9.3e+03	8.7e+03	1.1e+04	7.8e+03	8.4e+03	2.1e+01	3.7e+02	8.5e+02
2000	$\mathcal{H}_\infty$ -norm	—	—	—	3.3e−01	3.1e−01	3.1e−01	3.9e−01	3.8e−01	3.8e−01
	runtime	—	—	—	1.7e+05	1.1e+05	8.7e+04	2.0e+01	5.2e+02	9.5e+02

- Mehrmann, V., Morandin, R., Olmi, S., Schöll, E., 2018. Qualitative stability and synchronicity analysis of power network models in port-Hamiltonian form. *Chaos* 28, 101102.
- Mehrmann, V., Unger, B., 2022. Control of port-Hamiltonian differential-algebraic systems and applications. Available at <https://arxiv.org/abs/2201.06590>.
- Mitchell, T., Overton, M.L., 2015. Fixed low-order controller design and  $H_\infty$  optimization for large-scale dynamical systems. *IFAC-PapersOnLine* 48, 25–30.
- Mitchell, T., Overton, M.L., 2016. Hybrid expansion-contraction: a robust scalable method for approximating the  $H_\infty$  norm. *IMA J. Numer. Anal.* 36, 985–1014.
- Mogensen, P.K., Riset, A.N., 2018. Optim: A mathematical optimization package for Julia. *J. Open Source Softw.* 3, 615–618.
- Moser, T., Schwerdtner, P., Mehrmann, V., Voigt, M., 2022. Structure-Preserving Model Order Reduction for Index Two Port-Hamiltonian Descriptor Systems. *arXiv Preprint arXiv:2206.03942*. Available at <https://arxiv.org/abs/2206.03942>.
- Mustafa, D., Glover, K., 1991. Controller reduction by  $\mathcal{H}_\infty$ -balanced truncation. *IEEE Trans. Automat. Control* 36, 668–682.
- O’Donoghue, B., Chu, E., Parikh, N., Boyd, S., 2016. Conic optimization via operator splitting and homogeneous self-dual embedding. *J. Optim. Theory Appl.* 169, 1042–1068.
- Oliveira, G.H.C., Rodier, C., Ihlenfeld, L.P.R.K., 2016. LMI-based method for estimating passive blackbox models in power systems transient analysis. *IEEE Trans. Power Delivery* 31, 3–10.
- Ortega, R., van der Schaft, A., Castaños, F., Astolfi, A., 2008. Control by interconnection and standard passivity-based control of port-Hamiltonian systems. *IEEE Trans. Automat. Control* 53, 2527–2542.
- Ramirez, H., Gorrec, Y.L., Maschke, B., Couenne, F., 2016. On the passivity based control of irreversible processes: A port-Hamiltonian approach. *Automatica J. IFAC* 64, 105–111.
- Ravanbod, L., Noll, D., 2012. Gain-scheduled two-loop autopilot for an aircraft. *IFAC Proc. Vol.* 45, 772–777.
- Robu, B., Budinger, V., Baudouin, L., Prieur, C., Arzelier, D., 2010. Simultaneous  $H_\infty$  vibration control of fluid/plate system via reduced-order controller, in: *Proc. 49th IEEE Conference on Decision and Control (CDC)*, Atlanta, GA, USA. pp. 3146–3151.
- Schwerdtner, P., Mengi, E., Voigt, M., 2020. Certifying global optimality for the  $\mathcal{L}_\infty$ -norm computation of large-scale descriptor systems. *IFAC-PapersOnLine* 53, 4279–4284.
- Schwerdtner, P., Voigt, M., 2020. SOBMOR: Structured Optimization-Based Model Order Reduction. *arXiv preprint arXiv:2011.07567*. Available at <https://arxiv.org/pdf/2011.07567.pdf>.
- Schwerdtner, P., Voigt, M., 2021. Adaptive sampling for structure-preserving model order reduction of port-Hamiltonian systems. *IFAC-PapersOnLine* 54, 143–148.
- Skogestad, S., Postlethwaite, I., 2005. *Multivariable Feedback Control*. 2nd ed., Wiley.
- Wang, F.C., Chen, H.T., 2009. Design and implementation of fixed-order robust controllers for a proton exchange membrane fuel cell system. *Internat. J. Hydrogen Energy* 34, 2705–2717.
- Werner, S.W.R., Overton, M.L., Peherstorfer, B., 2022. Multi-fidelity robust controller design with gradient sampling. *arXiv preprint arXiv:2205.15050*. Available at <https://arxiv.org/abs/2205.15050>.
- Zhang, M., Borja, P., Ortega, R., Liu, Z., Su, H., 2017. PID passivity-based control of port-Hamiltonian systems. *IEEE Trans. Automat. Control* 63, 1032–1044.
- Zhou, K., Doyle, J.C., Glover, K., 1996. *Robust and Optimal Control*. Prentice-Hall, Englewood Cliffs, NJ.